ANALYSIS OF SABANCAYA VOLCANO, SOUTHERN PERU USING RADARSAT AND LANDSAT TM DATA.

Mark Bulmer, Andrew Johnston and Frederick Engle
Center for Earth and Planetary Studies, National Air and Space Museum, Smithsonian Institution, Washington D.C., USA 20560-315
Phone: (202) 633-9896 Fax: (202) 786-2566
E-mail: mbulmer@ceps.nasm.edu

Abstract
The geology and surface morphology of Sabancaya volcano are investigated using a combination of RADARSAT, Landsat Thematic Mapper (TM) and field observations. The morphology of the volcano is dominated by a summit dome and the currently active cone, both surrounded by blocky lobate lava flows. Forty two different volcanic flows are identified from geologic mapping, thirty nine more than previously recognized. The summit dome and cone are the main source vents for these flows. Sabancaya volcano, located 70 km northwest of the city of Arequipa has had five recorded eruptions since 1750. In 1986, the volcano again became active. Eruptions began in 1988 and continued until 1996. In August and September 1998, we observed small ash eruptions and increased gas emissions from the crater compared with the previous two years. This confirms that there is a need for further monitoring of the volcano. In 1997, a new project was begun to study Sabancaya volcano. As part of this, RADARSAT data are combined with a range of other remote sensing images to determine the geological history of the volcano and the natural hazards it poses to those living within its sphere of influence. Until 1990, much of the volcano was hidden from view by a permanent ice field. As a consequence of ash induced melting this ice has now largely been removed, but that which remains at the summit continues to pose a hazard. The RADARSAT image acquired in 1997 shows for the first time the complete lava flow complex at Sabancaya. Using this image we have constructed a detailed geological map of the lava flows at Sabancaya and have identified many flows unrecognized in previous maps [Klinck et al., 1986; Guillande et al., 1992; Thouret et al., 1995]. We have derived a general stratigraphic sequence of flows and re-evaluated the eruptive history of lava's at Sabancaya.

Introduction
Sabancaya volcano (15.47°S, 71.51°W) lies within the high Puna plateau and forms a part of the Cordillera Occidental; a NW-SE trending mountain range with peaks over 6000 m. The volcano is part of a complex which consists of Nevado Ampato (6299 m) to the south and Hualca Hualca (6025 m) to the north (Figure 1). Five eruptions have been recorded at Sabancaya since 1750 [Ceresis, 1989;

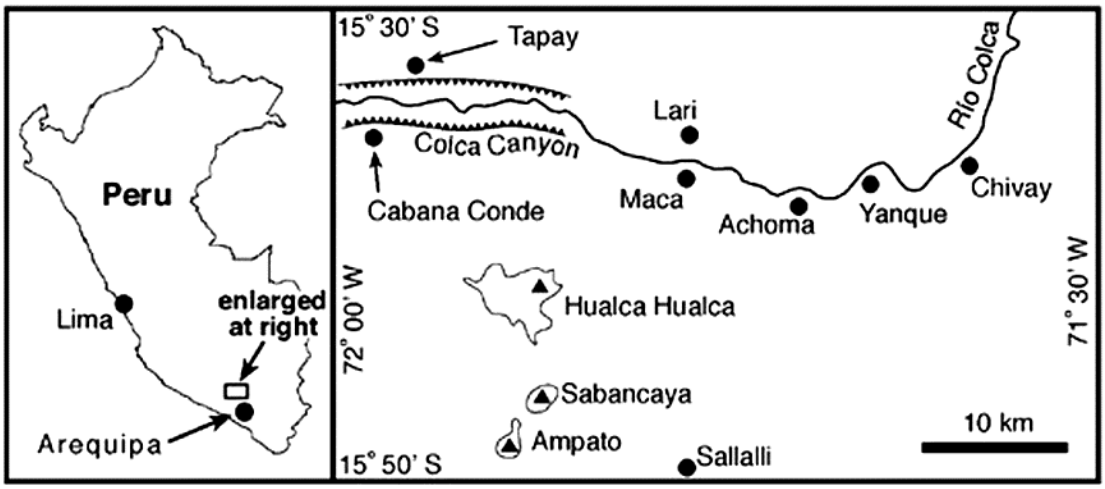

Figure 1. Location of the study site, selected towns in the Colca Valley, and the farmstead of Sallalli.

Simkin et al., 1981; Huaman, 1988, 1989, 1990]. After approximately 200 years of dormancy the volcano began erupting in the late 1980's and continues to be active. Due to the relative remoteness and inaccessibility of Sabancaya, much of what is known about the volcano has been derived from the interpretation of remote sensing data. Changes in crater area and shape are visible in Landsat TM images from the mid to late 1980's [DeSilva and Francis, 1991]. SPOT images were used by Chorowicz et al. [1992] and Guillande et al. [1992] to examine morphological changes on the volcano during the period of activity 1986-1990. Thouret et al. [1995] also used SPOT imagery to map volcanic activity and evaluate hazards at Sabancaya. To understand the geological history of the volcano, it is important to conduct detailed studies of the morphologies, distributions and stratigraphic relations of the volcanic deposits. In this paper, we use a combination of remote sensing datasets and field observations to characterize the volcano. Much of the work done on the volcano which covers the on-set of the main eruptive period 1990-1991. This work utilized SPOT images, and concluded that Sabancaya poses a potential threat to local communities and the 25,000 people in the Colca Valley [Thouret et al., 1995]. Since the early 1990's there has been no coherent program to monitor the volcano.

To characterize the volcanic and tectonic features which comprise Sabancaya, we use RADARSAT and Landsat TM images. RADARSAT is the primary tool for unit definition and geological mapping. Field observations along with other remote sensing data provide a guide to the interpretation of the RADARSAT and TM images. By using the remote sensing data combined with the field observations, we have addressed the following questions; (1) what are the distributions of volcanic products, (2) where are the source areas, (3) what are the surface morphologies of the flows, and (4) what is the general stratigraphic sequence. We have recently collected field topography profiles on one of the lava flows which will better guide the interpretation of the RADARSAT data. However,

we restrict ourselves to the interpretations based primarily on mapping using RADARSAT and TM, and leave analysis of the roughness of surface materials for future presentation.

Remote Sensing Data

There is a unique remote sensing database for Sabancaya from both airborne and spaceborne sensors which covers the period prior to the onset of new activity to the present. Images available include: aerial surveys from 1955 and 1977; occasional Space Shuttle 70 mm images from the mid 1980's; Landsat Multispectral Scanner (MSS) and Landsat TM; selected SPOT dates; ERS-1 and 2 and now RADARSAT. Each of these provides slightly different information about the same area. Prior to our analysis, Sabancaya had not been examined using the microwave portion of the electromagnetic spectrum. We used the RADARSAT scene collected on 26 August 1997, to examine the physical properties of the volcano. The radar image is single look right-looking fine beam mode (FR4) at 44.70° incidence angle, HH polarized. An area 57 x 37 km is covered at a resolution of 6.25 m/pixel. The image was processed so that it is aligned along the ascending orbit track and has been corrected for systematic errors related to satellite movement, the SAR instrument and processor, and data reception [RSI, 1995]. The single look RADARSAT data has a high signal-to-noise ratio making it appear grainy (Figure 2). We averaged the data by 2 to create a four-look image (Figure 2b). The reduction in the signal-to-noise ratio leads to a loss in resolution but features such as the lava flows can be better distinguished in the four look image than in the 1-look. It is possible the C-band 5.6 cm wavelength used in the RADARSAT system to delineate very subtle textural changes in geologic surfaces. Radar images have successfully been used to determine different physical properties of lava flows [Campbell and Shepard, 1996] and rocky debris avalanche deposits [Bulmer and Guest, 1996].

We used Landsat TM data to provide a regional context to our study of Sabancaya and to constrain radar image geometry as well as backscatter models. The TM image used for this study was collected in September 1986 by Landsat 5 and covers the entire area between the Colca Valley and Arequipa. The image was georeferenced using control points collected during field work in 1997. Both the TM and RADARSAT images were referenced to UTM coordinates using a second order polynomial. TM data allowed for the visual interpretation of surface structure of lava flows (Figure 2c). TM bands 4 and 1 were found to be the most useful channels for this task because contrast between flow features was highest in these bands. Vegetation at the margins of the flows is highly visible in the band 4 data.

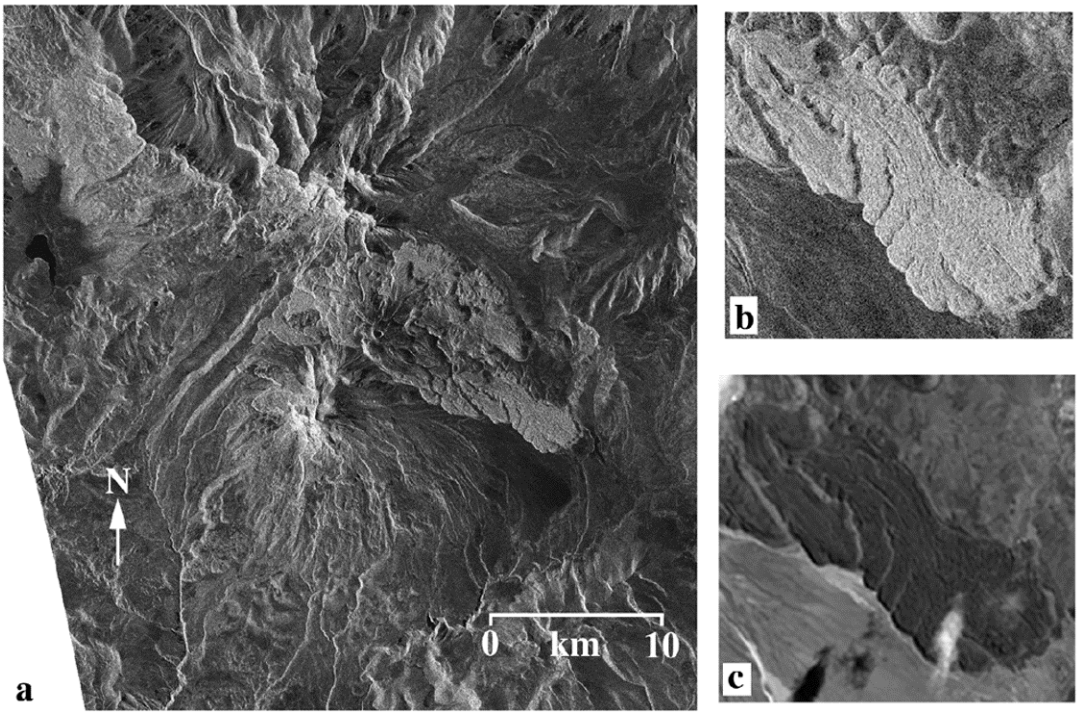

Figure 2. RADARSAT and Landsat TM image of Sabancaya volcano (a) shows 1 look full resolution (6.25 m) SAR image of the cone and lava flows at Sabancaya, with Ampato to the south and to the north the southern flank of Hualca Hualca, (b) shows a 4 look image (12.5 m resolution) of flows on the eastern flank of the volcano, (c) shows the same flows in the TM image.

Regional geology of Sabancaya

Utilizing both Landsat TM and a near-vertical space shuttle 70 mm image we have identified at least seven volcanic cones (500 m in diameter) within 50 km of Sabancaya. As well as these cones, four stratovolcanoes occur 70 km to the southeast which have the same N-S alignment as Ampato, Sabancaya and Hualca Hualca. The best known of these volcanoes are Chachani and Misti. Two volcanoes in the region have morphologies similar to those at Sabancaya; one to the northwest on the opposite side of the Colca valley, and the other situated at the base of Chachani. Ampato, Hualca Hualca, and Sabancaya volcanoes are built on late Tertiary and Quaternary volcanics formed from andesites, dacites, and ignimbrites [Klinck et al., 1986]. Ampato is composed of at least three lava domes aligned N-S, the oldest being to the south. A thick sequence of post-glacial tephra and volcaniclastic deposits occur around the eastern flank of Ampato and welded scoria flows on the SE flank provide evidence of explosive activity either from Ampato and/or Sabancaya. Glacial dissection by an ice surge which most likely occurred during the Holocene period, has resulted in some modification of Ampato and morraines are well preserved on the lower slopes of the west flank. Hualca Hualca, to the north of Sabancaya sits on the southern margin of the Colca Valley. During the Pleistocene a massive sector collapse on the northern flank blocked the

Colca river. This caused a lake to form upstream as far as the town of Chivay (Figure 1). On the north flank of Hualca Hualca near to the upper catchment of the Rio de Hualca Hualca a small parasitic volcano called Cerro Ahuashune has been constructed which is surrounded by blocky flows.

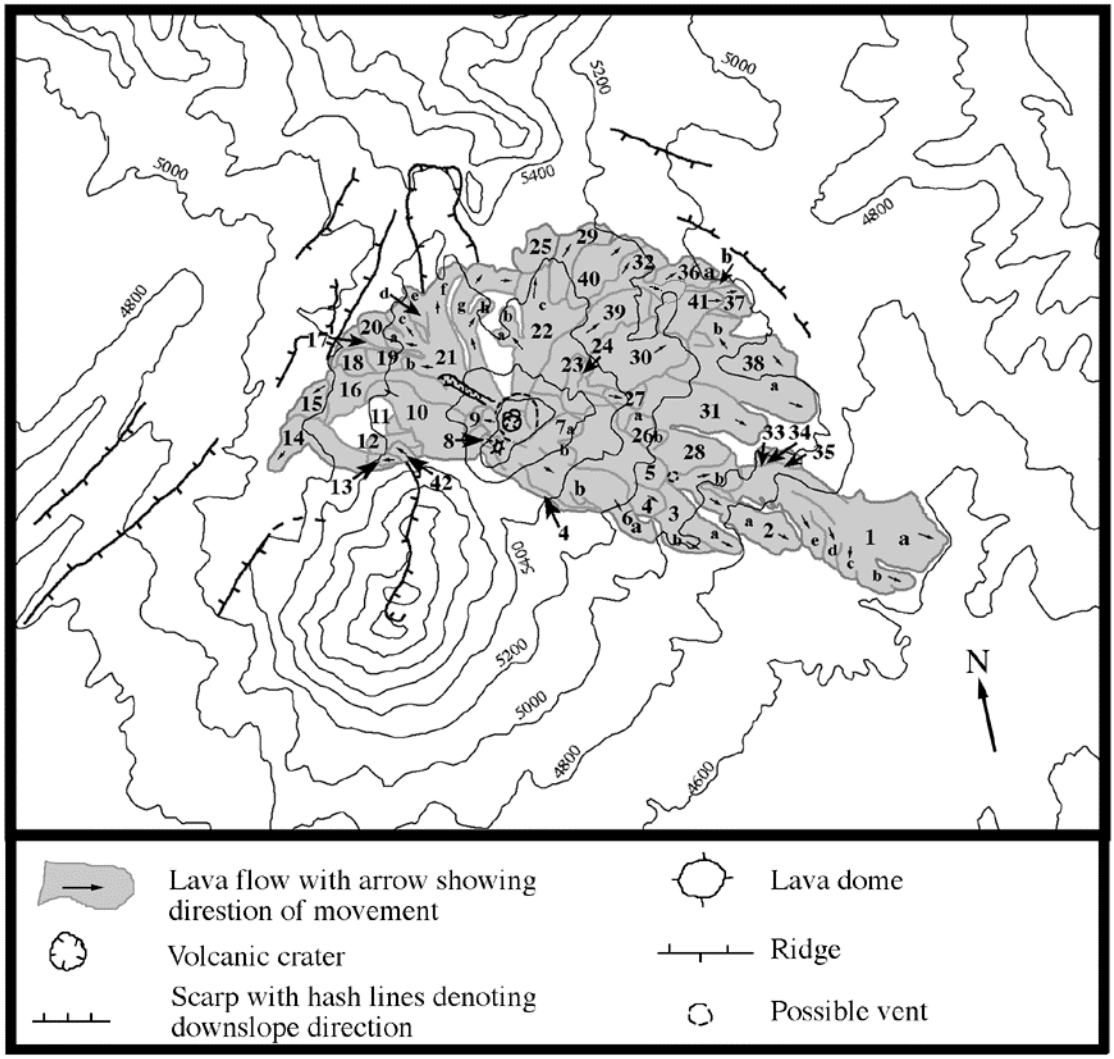

Figure 3. Preliminary geological map of Sabancaya derived from the 1997 RADARSAT image. Lava flow locations with their designated numbers are overlain by contours derived from the Instituto Geografico National 1:100,000 Chivay map sheet. Elevation in meters.

To assess the sequence of events and styles of volcanism at Sabancaya we produced a geological map (Figure 3). The resolution of the RADARSAT data permits stratigraphic and structural interpretation. Unit boundaries were defined on the basis of morphological, textural, and structural characteristics visible in the radar images. The units have been placed in a tentative age sequence based on superposition and cross-cutting relations. Sabancaya is situated between Ampato and Hualca Hualca and is the youngest strato-volcano in the cluster. Of the three volcanoes it is the only one that has been historically active. Sabancaya is

approximately 16 km in diameter, and covers an area of 68 km^2 which is characterized by a summit dome and the currently active cone, both surrounded by thick lobate lava flows. The summit cone and dome are the two main source vents. The surface of the lava flows is dominated by meter sized blocks and strong backscatter coefficients on the flows (Figure 2b) arise due to their roughness at the sensor wavelength combined with highly irregular local relief. We discuss each of the mapped units below.

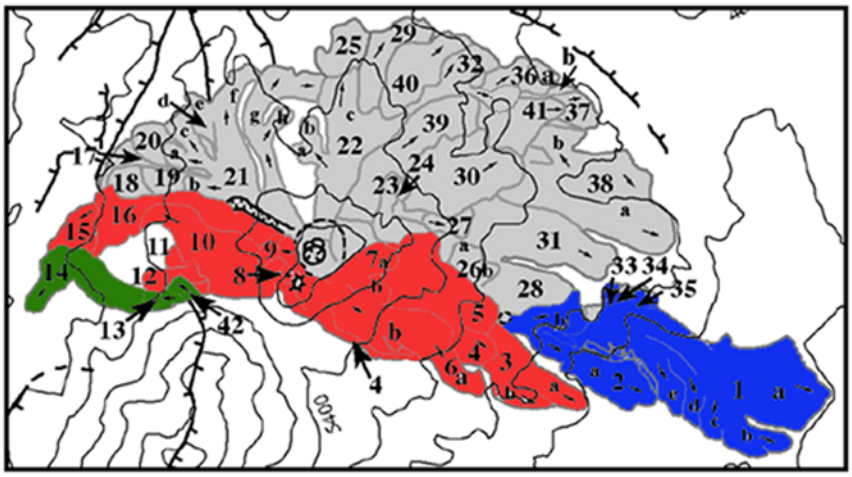

Figure 4. Color map showing the origin of flows at Sabancaya. Flows from: Ampato are green, the dome vent at Sabancaya are red, the cone vent are gray, and the suggested flank vent are blue.

Summit dome

A lava dome (5976 m asl) occurs 800 m to the south of the ash cone, close to the flanks of Amapto (Figure 2 and 3). The image geometry of the RADARSAT data make it difficult to determine the shape of the dome which is symmetrical and covered with ice over which is an ash layer. The dome is older than the vent over which the current cone is being built if the eruptive activity at Sabancaya has migrated northward similar to that which occurred on Ampato. Lava flows such as 8, 10, 11, 12, 15 plus 16 to the west, and 3,4 as well as 6 on the eastern flank likely originated from the vent over which this dome was emplaced (Figure 3 and 4). On the west flank, flow 15 is the oldest and its flow path was diverted by a topographic barrier causing it to follow a course to the southwest. Guillande et al. [1992] mapped this flow as originating from Ampato but in the remote sensing data we find no evidence to support this. Superposed on flow 15 is 16 which is 3 km long and 1.5 km wide at the distal margin. Flow 10 overlies 16 as well as 11, 12 and 42. Flows 12, 13 and 14 all appear to have originated from the north dome of Ampato. This may also be true for flow 42. The age sequence from oldest to youngest for these flows from Ampato is 14, 12, 13 and 42. Similar to flow 15, 14 was diverted to the southwest. Flow 14 overlaps 15 from Sabancaya indicating that if 14 originated from Ampato then eruptive activity from the two vents overlapped for a period. A lobe on the southern margin of flow 10 overlies 42 which is youngest the flow from Ampato. This indicates that flow 10 is younger than all of the flows on the northwest flank of Ampato.

On the east flank, the age sequence of flows from oldest to youngest is 1?, 33, 34, 35, 31, 28, 26, 2?, 3, 5, 4, 7, and 6. With the possible exception of flows 1 and 2 we interpret these flows as having originated from the dome vent. Flow 1 covers an area of 7.4 km^2 and has five distinctive lobes. The flow has an average thickness of 60 m and slope angles on the margins ranging from 32 to 37 . The longest portion of the flow 1a has a length of 4.9 km and is 1.8 km wide at the distal end. The initial travel path of the flow appears to have been towards Sallalli (Figure 3). Surface structures such as levees and channels which are longitudinal to the flow direction as well as pressure ridges which are perpendicular to it, are well defined on the flow. Flows 33, 34 and 35 on the north side of 1a (Figure 3) were likely lobes off the main flow which filled topographic lows. There are a series of levees on the northern margin of flow 1, and a channel in the main body which seems to have deflected lobe 1b off to the southeast (Figure 2b, c). This resulted in the series of lobes 1c, d and e being formed in the latter stages of the eruption. The youngest of these is 1e. The travel paths of each was dictated by lobe 1b. We suggest two scenarios for the origin of flow 1: (1) that the tapering of the proximal part points to a source vent nearby, or (2) the tapering is a function of the topography over which it traveled and that its source was higher up the slope at the dome vent. Based on the available remote sensing data we favor the first scenario, that it originated from a nearby vent and that the majority of the flow is visible. Emplaced on top of flow 1 is 2 which has two lobes both with arcuate ridges perpendicular to the downflow direction and ridges which are longitudinal to it.. The lengths of 2a and 2b are 3.5 km and 1.6 km respectively and have slope angles on the flow margins ranging from 32 to 38 . The two lobes combined cover an area of 0.9 km^2. Based on the tapering and thinning of the proximal zone of the flow we suggest that it may have had its own source area and that it was the same one that produced flow 1 (Figure 3 and 4). If this is true then it is hard to place flow 1 and 2 in a general age sequence. The stratigraphic relation between lobe 2a and 1e is not clear. The distal zone of 2a is 107 m thick compared with only 60 m for 1e side [Bulmer et al., 1998]. The nature of the flow front at 2a is such that two possibilities exist: (1) the distal part of 2a lies on 1e, or (2) that 2a flowed along the edge of 1e and does not rest on it. Based on its superposition relations flow 2 is younger than flows 1 and 39. Flow 2 is younger than flows 31 and 28. The age sequence between flows 3 and 2 is uncertain but the former is thicker and has fewer but larger arcuate ridge structures than the latter. Superposed on flow 3 are flows 4 and 5. Flow 4 is younger than 5. The age sequence of flow 26 relative to that 5 is uncertain. Lying on top of flows 4 and 7 is 6 which we interpret to be one of the youngest from the dome vent. It is 4.2 km long, 0.64 km wide at the distal zone and covers an area of 3.2 km^2. This flow traveled off the side of 4 and onto the pampa.

Summit cone

The cone, situated at 5976 m asl. has a diameter of 1 km, is 170 m high and covers an area 0.09 km^2. The current ash cone is being built over an older vent from which lava flows to the west, north, and east appear to have originated

(Figure 4). To the west, flows interpreted to have been erupted from the cone vent, listed in age sequence from oldest to youngest are 17, 18, 19, 20, and 21 (Figure 3). Flow 17 appears to have spread at the distal zone due to its forward motion being impeded by the same topographic barrier which diverted flows 15 and 14. The age relation between flows 17 and 16 is not clear. Flow 18 lies on 17 which in turn is superposed by 19 and is younger than 16. It may be that flows 19 and 20 are contemporaneous. Overlying flows 19 and 20 is 21 which can be traced back to the cone vent. This flow appears to have bifurcated into 8 separate lobes most likely in response to the surface over which they traveled. The travel paths of lobes 21f, g, and h were constrained by the flanks of Hualca Hualca.

To the north of the cone vent the most prominent lava flow is 22 which can clearly be sourced back to the vent. The oldest flow to the north is 25 which has pronounced ridges perpendicular to the movement direction. It is overlapped by flow 40 which in turn has 29 superposed on it. These flows appear to have had their travel distance constrained by a break of slope caused by deposits from Hualca Hualca. The main part of flow 22 traveled over the upper reaches of 25, 40 and 29.

On the northeastern side of the cone the age sequence from oldest flows to youngest is 36, 37, 41, 32, 39, 24 and 23. Flows 23 and 24 are emplaced over 39. Flows 32, 37, and 36 were constrained by a break of slope related to deposits from Hualca Hualca. Near to the distal zone of 36 there is a sequence of overlapping flows, the sequence from oldest to youngest being 36, 37, 41 then 32. On its southern margin lavas from flow 36 are superposed on a lobe from 38. This indicates that flow 36 is younger than 38. Well developed levees occur on the northern margin of flow 38 and appear to have formed in response to the lava moving in a progressively more southerly direction. The reason for this change in direction was likely a response to the constraining slope to the east (Figure 3). An age sequence from flow 38 to the cone vent can be determined. From oldest to youngest it is 38, 31, 28, 27/26, 30, 5, 23. Flow 23 actually forms a lava ridge connecting to the cone vent.

At the summit vent the current ash cone dates from the late 1980's. Fumarolic activity began at the summit in December 1986, and progressed to large ash eruptions in May 1990. Fumarolic activity caused the ice to melt revealing the current crater in 1989. There are at least three coalesced craters at the summit. They occur on the north and west sides of the current crater which has a diameter of 410 m (Figure 3). An examination of the cone on 10 August 1987, revealed gas emission from several sources in a moat surrounding a central plug in the crater [SEAN Bulletin, v.13, no.6, 1990]. In June 1988, snow around the summit area was mantled with ash. The main eruptive phase began 29 May, 1990 when ash plumes rose to heights of 3-6 km and glowing tephra was reported. In June 1990, tens of centimeters of ash were reported on the summit of Sabancaya [SEAN Bulletin v.15, no.6, 1990]. Using SPOT data, Chorowicz et al [1992] noted tephra covered the ice cap had black or light gray radiometric signals which expressed differences in ash thickness and in surficial melting. The backscatter cross sections of ash deposits in the RADARSAT image have yet to be studied. Tephra erupted in 1990 had 10-20% phreatomagmatic deposits suggesting limited magma

water interaction. Lithic products were 80-80% in October. These lithics are gray, often weathered fragments of dacite. By 1992, 20% of the ballistic blocks being ejected were vitreous, vesiculated and have radial fractures supporting the idea that a magmatic intrusion was rising in the conduit. In December 1992, the juvenile component in the tephra had increased to 40-50% indicating much of the older capping rock had been removed (G. Salas, pers. comm.). The juvenile material consists of black, vitreous and unweathered fragments which are andesitic and dacitic (58-63% SiO_2). We are unaware of any analysis of ash compositions erupted in the past four years. In 1998, there has been an increase in the amount of gas being emitted over the previous year and ash eruptions were observed in August and September. To-date we have not been able to image the floor of the crater to look for evidence of a plug.

Summary

Using RADARSAT and Landsat TM data it has been possible to geologically map the distribution of lava flows around Sabancaya. We have identified two main source vents as well as a possible parasitic vent on the east flank. This has further constrained the geological history of the volcano and the products which have been erupted. The lava flows at Sabancaya have distinctive lobate morphologies and well defined flow fronts. Their morphologies are similar to those at Chao, Chile [Guest and Sanchez, 1969]. We have mapped 42 separate flows and 59 flow lobes which we have placed in a tentative stratigraphic sequence. We suggest that the flows can be traced to two known source vents at the summit and one suggested flank vent. Based on superposition relations, flows from the dome vent are interpreted to be older than those from the cone vent. On the west side of the dome vent, flows from Sabancaya can be sequenced with lava flows from Ampato. We find that the eruptive histories of lavas from the north dome of Ampato and the dome vent at Sabancaya overlapped in time. On the east flank we suggest that flow 1 and 2 originated from a parasitic vent and that flow 1 is younger than nearby flows from the cone vent.

Based on the geological map it is apparent that lavas have erupted frequently at Sabancaya since the Holocene. The relatively short distance that these flows have traveled indicates a new flow would only pose a geohazard to farming settlements near to the volcano. A greater hazard is posed by ash which has contaminated grazing and induced melting on the glaciers on Ampato and Hualca Hualca as well as on Sabancaya, which caused mudflows from 1990-1991. Increased knowledge of the eruptive history at Sabancaya is vital to any assessment of the potential hazards associated with the active volcano and the risks they pose to the peoples living within the sphere of influence.

Acknowledgments

The authors would like to thank Guido Salas and Bruce Campbell for useful discussions. We would also like to thank RADARSAT International. This work was funded through the Garber Fellowship, Smithsonian Women's Committee, Honda Corporation and NASA Stennis Commercial Remote Sensing Center.

References

Bulmer, M.H. and J.E. Guest, 1996. Modified volcanic domes and associated debris aprons on Venus, in W.J. McGuire, A.P. Jones and J. Neuberg, eds., Volcano Instability: Spec. Pub. Geol. Soc. Lond**,** 110, pp.349-371.

Bulmer, M.H. , F.C.., Engle, A.J., Johnston, and H., Bulmer, 1998. Topographic surveying on Sabancaya volcano, southern Peru. Submitted to American Geophysical Union, Fall San Francisco.

Campbell, B.A. and M.K. Shepard, 1996. Lava flow surface roughness and depolarized radar scattering, J. Geophys. Res., 101:18,941-18,951.

Ceresis, 1989. Riesgo volcanico: avaluacion y mitigacion en America Latina. Aspectos sociales, institucionales y cientificos, Centro Regional del Sismologia para America del Sur. Lima, 298 p.

Chorowicz, J., B. Deffontaines, D. Huaman-Rodrigo, R. Guillande, F. Leguern and J.-C. Thouret, 1992. SPOT satellite monitoring of the eruption of Nevado Sabancaya volcano (southern Peru), *Remote Sensing of Environment,* 42:43-49.

DeSilva, S.L., and P.W. Francis, 1991. Volcanoes of the Central Andes, Springer-Verlag.

Guest, J.E. and J.R. Sanchez, 1969. A large dacitic flow in northern Chile, Bull. Volcanol., 33:3, 778-790.

Guillande, R., J-C. Thouret, D. Huaman, F. Le Guern, R.M. Chevrier, et al., 1992. L'Activite eruptive actuelle de volcan Sabancaya (Sud du Pérou) et l'evaluation des menances et des risques: Geologie, cartographie et imagerie satellitaire, Guillande, R., J-C. Thouret, eds. Rapport Délégation aux Risques Majeurs, Minist. l'Environ, Paris, 133p.

Huaman, R.D., 1988. Primera expedicion de campo al volcan Sabancaya. Inf. Int. IGP., 4p.

Huaman, R.D. 1989. Exploitation des donnees SPOT pour l'analyse géoloogique et la localisation du risque naturel dans la vallée du Colca (Arequipa, Pérou). Rapport des DESS de télédetection, methodes et applications, GDTA. University Paris VI, 30p.

Huaman, R.D. 1990. Estudio del peligro geologico en la zona del volcan Sabancaya: Los megadeslizamientos de la margen derecha y las partes altas del calle del Colca (alrtededores de Maca Pampa y Madrigal). Inf. Int. IGP. 8p.

Klinck, B.A., R.A. Ellison and M.P. Hawkins, 1986. The Geology of the Cordillera Occidental and Altiplano West of Lake Titicaca, Southern Peru, British Geol. Surv. Open File Rep., pp. 353.

RSI, 1995. RADARSAT Illuminated, Canada.

SEAN, 1990. Sabancaya report, In Bulletin Global Volcanism Network, 13:6, 10-12.

SEAN, 1990. Sabancaya report, In Bulletin Global Volcanism Network, 15:6, 2.

Thouret, J.-C., A. Gourgaud, M. Uribe, A. Rodriguez, R. Guillande and G. Salas, 1995. Geomorphological and geological survey, and spot remote sensing of the current activity of Nevado Sabancaya stratovolcano (south Peru): assessment for hazard-zone mapping, Zeitschrift Geomorph. N.F., 39:4, 515-535.